

# LOSSLESS MAGNETIC BEARING BY MEANS OF SMOOTHED FLUX DISTRIBUTION

Nobuyuki Kurita, Ryou Kondo and Yohji Okada

Department of Mechanical Engineering, Ibaraki University, Hitachi, Ibaraki-Pref., 316-8511 Japan  
 hkurita@mech.ibaraki.ac.jp, kondo@mech.ibaraki.ac.jp, okada@mech.ibaraki.ac.jp

## ABSTRACT

For high speed and long-term rotor such as an energy storage flywheel, eddy current in the laminated steel sheet causes rotating loss. In this paper, a new type of magnetic bearing is proposed which has smooth flux distribution. The rotating loss is expected to be negligible, while it has high force factor due to high bias flux produced by permanent magnets. To confirm the operation of the proposed magnetic bearing, a simple experimental setup was fabricated and tested. The results showed smooth rotation with a low vibration level. Free-run test was carried out to clarify the rotating loss. The test results are compared with the standard magnetic bearing of the same size.

## INTRODUCTION

The demand of electric power consumption increases in daytime while it remains low level in nighttime. The electric power plant is better to operate constantly. The efficiency of electric power plant will be improved, if the power is stored effectively. An energy storage flywheel is considered as one of the most efficient methods [1]. The flywheel is accelerated by an electric motor at night using surplus power while it regenerates electric power in daytime. Hence, such a flywheel should pass the critical speed and keep high-speed rotation between nighttime and daytime. Recently, such a flywheel has been developed and reported [1],[2]. Magnetic bearings are used to support the flywheel, because it is considered without any friction. For the usual application, eddy current loss is drastically reduced by using laminated steel sheets. For such a high speed and long term application, however, the eddy current loss in the laminated steel sheet is still induced.

This paper proposes a new type of magnetic bearing which is expected to have almost zero eddy current loss. The proposed magnetic bearing is based on the hybrid type one, which has high bias

flux produced by permanent magnets. The stems have long feet between them to smooth the flux distribution [3]-[5]. Control flux is relatively low level. Hence the flux distribution is smooth in the rotating circumference to avoid the eddy current. Experimental setup was made to confirm its basic characteristics. To realize high stability a centralized control was adopted to the experimental setup. Free-run test was carried out to clarify effectiveness of the proposed magnetic bearing. The results are discussed in detail.

## LOSSLESS MAGNETIC BEARINGS

Standard magnetic bearing has the concentrated pole stems, which are magnetized N or S poles by turns, as shown in Fig. 1. Eddy current is induced in the rotor when it rotates in such a sudden flux change. The magnetic bearing is usually considered without any rotating loss. However, for high speed and long-term application eddy current loss in the rotor causes serious problem. In addition, standard magnetic bearing requests bias flux to linearize the magnetic force. Thus, power consumption is high.

### Proposed radial magnetic bearing

The proposed magnetic bearing can reduce the eddy current loss by means of smooth flux distribution [4],[5]. The schematic of proposed magnetic bearing is shown in Fig. 2. It has 6 poles the top of which has long feet to smooth the flux distribution. The sinusoidal flux distribution is expected by giving the quasi-sinusoidal currents into each coils, as shown in the lower part of Fig. 2. Additionally, airgap of the rotor and the stator is designed relatively wide of 1 [mm] to smooth the flux change. Regardless of wide airgap, strong bias flux is produced by the rare earth permanent magnet. Operation of proposed magnetic bearing is the same as hybrid type one. When rotor is displaced, one side of the flux is decreased while the other side of

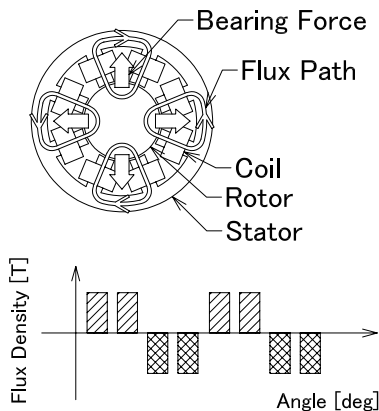


FIGURE 1: Schematic of Standard Magnetic Bearing

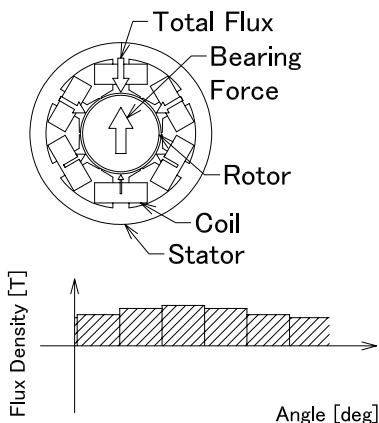


FIGURE 2: Schematic of Proposed Magnetic Bearing

the flux is increased by control current to correct the rotor displacement.

The stator is designed using the magnetic field analysis “ANSYS”. Analytical results of flux flow line is shown in Fig. 3 [4]. The bias flux flows in the airgap between the rotor and stator where the smoothed flux distribution is recognized.

**Integrated axial magnetic bearing**

The attractive force of the radial magnetic bearing stabilizes the axial motion passively. But the passive damping is poor causing serious problem for high-speed rotation. To overcome this problem an axial magnetic bearing has to be installed. However, additional actuator increases system complexity and shaft length. A new type of integrated axial magnetic bearing is introduced. The operational principle of the axial bearing is shown in Fig. 4. The left figure shows a cross section of the radial magnetic bearing. A cylindrical stator coil for axial magnetic bearing is installed in the

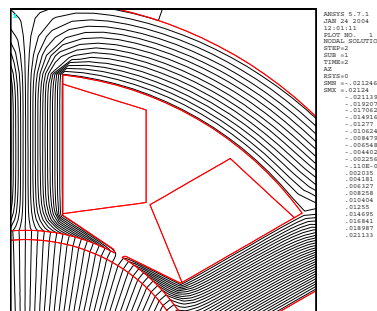


FIGURE 3: Analytical Result

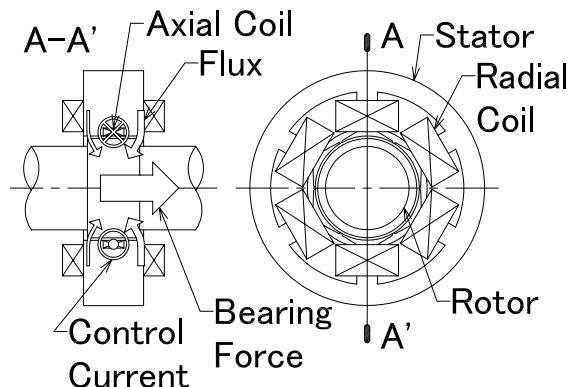


FIGURE 4: Operation of Integrated Axial Magnetic Bearing

middle of stator ditch. The stator width is designed wider than that of the rotor, hence the radial bias flux by permanent magnet has an axial component. The axial coil current is controlled according to the rotor axial displacement. One side of the flux is increased while the other side of the flux is decreased to create the axial force.

**EXPERIMENTAL SETUP**

To confirm the basic characteristics of the proposed magnetic bearing the experimental setup is made as shown in Fig. 5. The rotor is set horizontally and the proposed magnetic bearings are arranged on both ends. The permanent magnet is put in the center of two radial magnetic bearings. The axial magnetic bearing is integrated inside the left radial magnetic bearing. Four displacement sensors are installed to detect the radial displacements and one sensor is installed to detect the axial displacement. A permanent magnet type AC motor is installed at the right end to drive the rotor. The back yoke of the motor rotates with the rotor, thus the eddy current of the motor yoke is not induced. The airgap in the radial direction is 1 [mm]. The touch down bearings are installed to avoid the direct contact of the rotor and the sta-

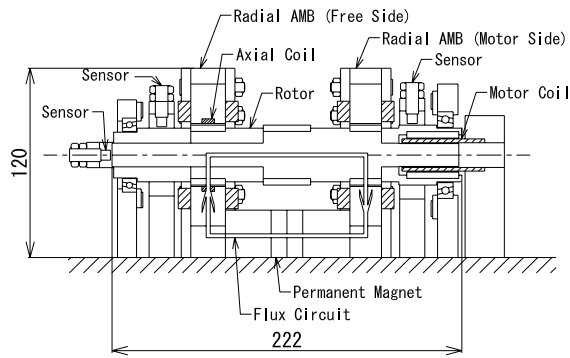


FIGURE 5: Schematic of Experimental Setup

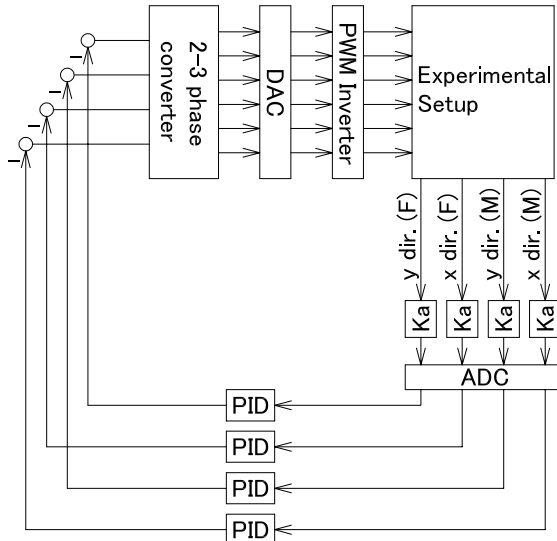


FIGURE 6: Schematic of Control System (Local Control)

tor. Hence the movable area is decreased to 0.5 [mm] in the radial and axial directions.

### Control System

Schematic of control system is shown in Fig. 6. The measured displacement signals are input to the computer via A/D converter and sent to digital PID controller to produce the actuating signals. Where local PID control is used. Then two-phase actuating signals are converted to three-phase signals and put out to PWM inverter via D/A converter. Where, y direction is defined as vertical and x direction is horizontal. Control gains of local PID control are determined experimentally and listed in Table 1. Where,  $K_p$  is the proportional gain,  $K_d$  is the derivation gain, and  $K_I$  is the integration gain, respectively. The derivative time constant used is 0.1 [msec] and the sampling interval is 0.1 [msec].

TABLE 1: Control Gains (Local control)

	Radial AMB	Axial AMB	unit
$K_P$	3000	4000	N/m
$K_D$	10	10	N s/m
$K_I$	1500	0	N/(m s)

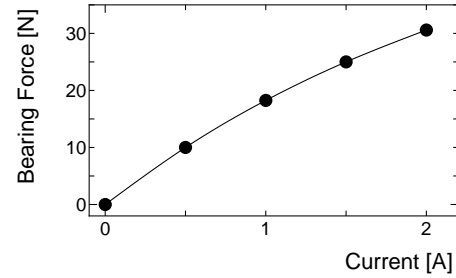


FIGURE 7: Bearing Force vs. Current

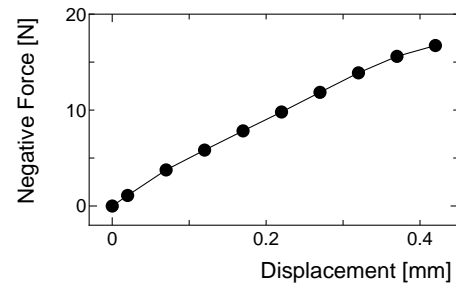


FIGURE 8: Negative Force vs. Displacement

### Static Characteristics

The bearing force and the negative force are measured to confirm static characteristics. The bearing force is measured using a spring balance when coil current increased form 0 [A] to 2 [A]. The results are shown in Fig. 7. Force factor is about 18 [N/A]. The rotor weight is 1.595 [kg]. The rotor can be supported by the control current about 0.3 [A] which is relatively low level.

The negative force of radial magnetic bearing is also measured using a spring balance when the rotor displacement changes from 0 [mm] to 0.4 [mm]. The results are shown in Fig. 8. The negative force coefficient is about 45 [N/mm]. Even if the rotor contacts to the touch down bearing, the negative force can be cancelled by the control current about 1.2 [A].

The bearing force and the restoring force of the integrated axial magnetic bearing are also measured. The results are shown in Figs. 9 and 10. The force factor of axial magnetic bearing is about 3 [N/A]. The restoring force factor is about 4 [N/mm]. From these results, axial magnetic bearing can provide enough damping to the rotor.

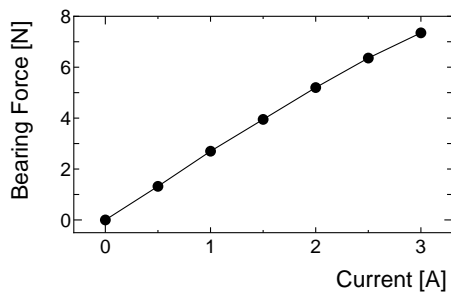


FIGURE 9: Bearing Force vs. Current

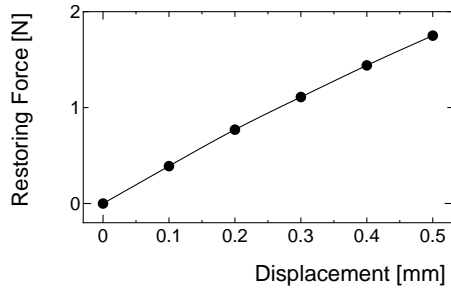


FIGURE 10: Restoring Force vs. Displacement

### Impulse Response

The impulse responses of the proposed magnetic bearing are measured and the results are shown in Fig. 11. Hammering force is added to free side of the rotor to produce about 0.2 [mm] displacements. After the hammering, the sensor outputs of four radial displacements are measured and recorded using digital oscilloscope. The rotor vibration decays within 0.01 [sec]. The stability is quite good. Moreover, there is low level interference between x and y directions. However, micro vibration of the rotor is recognized after the transient.

Similar experiments are carried out in axial direction. The results are shown in Fig. 12. Where (a) is the result without control and (b) is that with active control. The rotor vibration remains until 9 [sec] without control while the active control can decay the rotor displacement within 0.5 [sec]. The bearing force is considered enough to reduce transient vibration.

### Levitated Rotation

The levitated rotating test is carried out. The results are shown in Fig. 13. The motor increases the rotating speed stepwise by 200 [rpm]. After the rotor has reached to the steady-state speed, the vibration amplitude is measured and recorded. The vibration increases from 2,000 [rpm] and the maximum vibration is recognized at 7,000 [rpm].

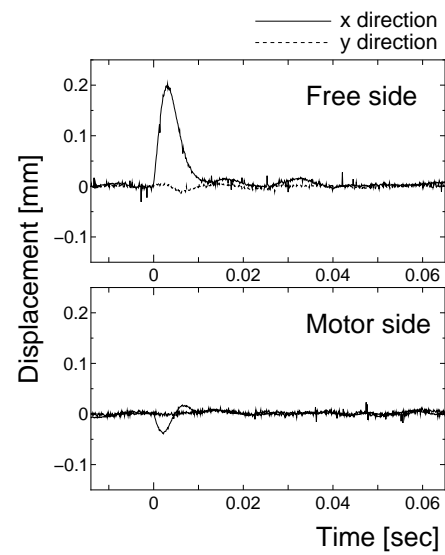


FIGURE 11: Impulse Response (Local Control)

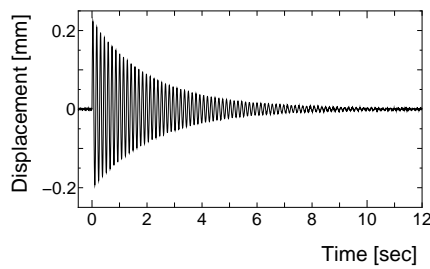
TABLE 2: Control Gains (Centralized Control)

Displacement	unit	
$K_P$	3000	N/m
$K_D$	10	N s/m
$K_I$	1500	N/(m s)
tilt		
$K_P$	300	rad/m
$K_D$	1	rad s/m
$K_I$	150	rad/(m s)

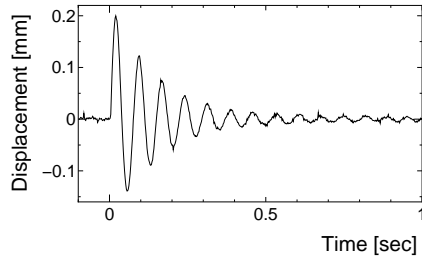
However, the amplitude of the rotor vibration is controlled under 0.02 [mm] for free side and 0.06 [mm] for motor side, respectively. The rotor could run up to 14,400 [rpm] without any serious problem.

### CENTRALIZED CONTROL

In order to improve the dynamic characteristics, the control method is changed from local control to centralized control. Schematic of control system is shown in Fig. 14. The measured displacement signals are input to the computer via A/D converter to calculate the central displacement and the inclination around the center of gravity. These signals are sent to digital PID controller and converted to the actuating currents. Then two-phase signals are converted to three-phase signals. After the conversion they are output to PWM inverter via D/A converter. Control gains of centralized PID control are determined experimentally and listed in Table 2.



(a) Without Control



(b) With Active Control

**FIGURE 12:** Impulse Response of Axial Magnetic Bearing

### Impulse Response

The impulse responses are tested by hammering the free side and recording the four displacements as shown in Fig. 15. Micro vibration of the rotor is suppressed compared with the local control. This is considered due to the perfect collocation of the sensor and the actuator. However, about 0.08 [mm] displacement is recognized in the motor side. Because, the rotor inclination is calculated from both side of the displacements which will affects adversely to the motor side displacement.

### Levitated Rotation

Unbalance response is measured by rotating the rotor at a constant speed and measuring the vibration amplitude as shown in Fig. 16. The maximum amplitude of the rotor is about 0.01 [mm] in free side and about 0.02 [mm] in motor side, respectively. The vibration level is reduced compared with the local control. The rotor could run up to 14,400 [rpm] with high stability.

### FREE-RUN TEST

In order to compare the rotating loss, the standard magnetic bearing is fabricated which has almost the same size of the proposed magnetic bearing. Previously free-run test in air was carried out [5]. However, there was no major difference between the standard magnetic bearing and the proposed magnetic bearing. Therefore, vacuum chamber is made and free-run test in vacuum is

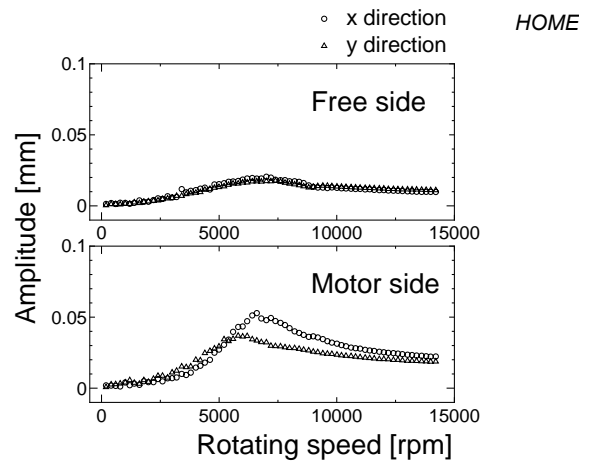


**FIGURE 13:** Unbalance Response (Local Control)

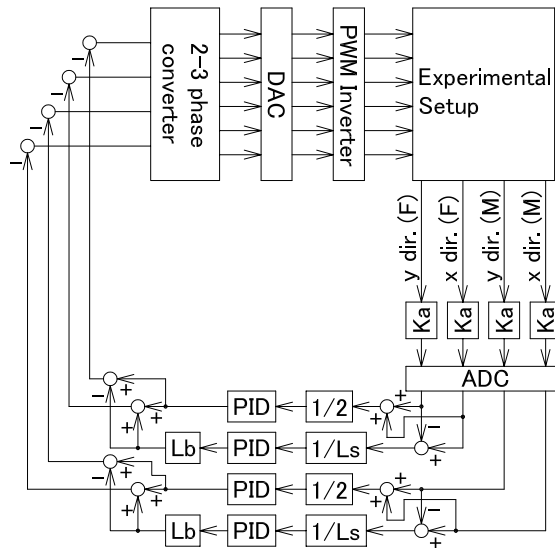


**FIGURE 14:** Schematic of Control System (Centralized Control)

carried out. The vacuum chamber is made of aluminum plates and sealed with silicone adhesive as shown in Fig. 17. The vacuum level is about 0.02 [torr]. The rotor runs up to 12,000 [rpm] by the motor. Then the power supply was disconnected and the deceleration characteristics were measured. The results are shown in Fig. 18. The running time of the proposed magnetic bearing is about 2.2 time longer than that of the standard magnetic bearing. This indicates that the proposed magnetic bearing can reduce eddy current loss.

However, the difference is not so big as expected on free-run test in vacuum. This is considered that the proposed magnetic bearing has the

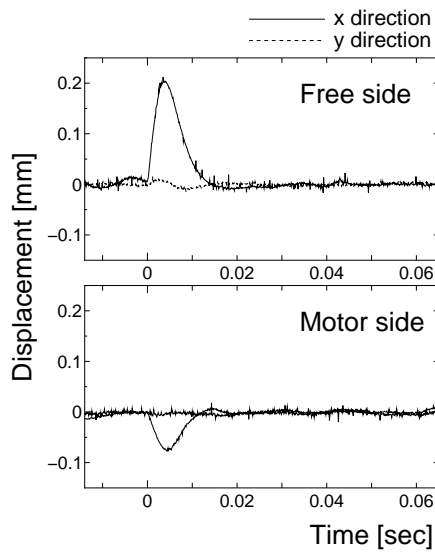


**FIGURE 15:** Impulse Response (Centralized Control)

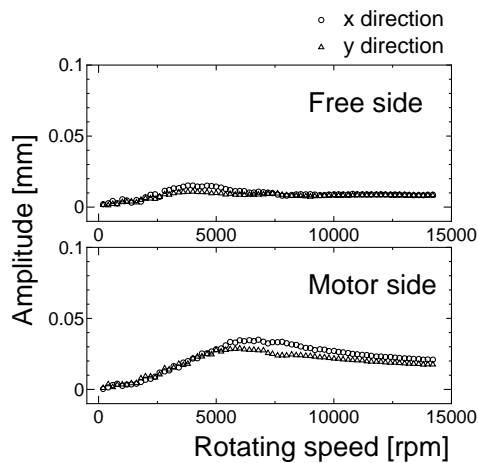


**FIGURE 16:** Unbalance Response (Centralized Control)

feet and the gap between the feet is about 1 [mm]. But, the flux distribution is not smooth completely because of these gaps. This suddenly flux change causes eddy current loss. Now the experimental setup is under modification for reducing rotating loss.

### CONCLUDING REMARKS

New type of radial magnetic bearing is proposed to reduce rotating loss. A new integrated axial magnetic bearing is also proposed. The experimental setup is fabricated and its fundamental characteristics are measured. The rotor can run up to 14,400 [rpm] with low level vibration.

The vacuum chamber is fabricated and free-

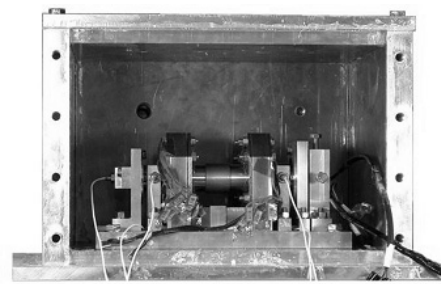


**FIGURE 17:** Photo of Vacuum Chamber

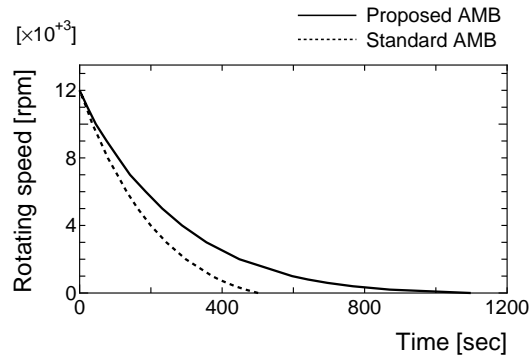


**FIGURE 18:** Free Run Test in Vacuum

run test is carried out. The proposed magnetic bearing indicates 2.2 time longer rotation than the standard magnetic bearing. Further works is continuing to reduce the rotating loss and increase the stability of the rotor.

### REFERENCES

1. Markus Ahrens, et. al.,: "Design of a Magnetically Suspended Flywheel Energy Storage Device", 4th ISMB, ETH Zurich, 1994, pp. 553-558.
2. Y.Miyagawa, et. al.,: "A Trial Manufacturing of Flywheel Energy Storage System", Preprint of Applied Superconductivity Conference, 1998.
3. Ha-Yong Kim and Chong-Won Lee,,: "Reduction of Eddy Current Loss in Small-Size Active Magnetic Bearing with Solid Cores and Rotor", 8th ISMB, Mito Japan, 2002, pp. 77-81.
4. Nobuyuki Kurita, et. al.,: "Development of Lossless Magnetic Bearing", 8th ISMB, Mito Japan, 2002, pp. 91-96.
5. Nobuyuki Kurita, et. al.,: "Development of Lossless Magnetic Bearing", The fifth Korea-Japan Symposium of Frontiers in Vibration Science and Technology, Suwon Korea, 2003, pp. 59-60.